Simultaneous Model Estimation and Image Reconstruction (SMEIR) to improve Multi b-Value body Diffusion-Weighted imaging

Moti Freiman[1], Onur Afacan[1], Robert V Mulkern[1], and Simon K Warfield[1]
[1]*Radiology, Boston Children's Hospital/Harvard Medical School, Boston, MA, United States*

Introduction: Diffusion-weighted MRI (DW-MRI) of the body is a non-invasive imaging technique sensitive to the incoherent motion of water molecules inside the area of interest. This motion is primarily characterized by a combination of a slow diffusion component associated primarily with the Brownian motion of water molecules, and a fast diffusion component associated primarily with the bulk motion of intravascular molecules in the micro-capillaries. The rapid DW-MRI signal decay in tissue combined with the reduced signal decay in regions of restricted diffusion increases the conspicuity of abnormal regions in DW-MRI images acquired with sufficiently high b-value and so can aid in detecting abnormal regions.

Unfortunately, DW-MRI images have an inherently low signal-to-noise ratio (SNR), which reduces enthusiasm for using these images for diagnostic purposes. Koh and Collins[1] recommend acquiring the DW-MRI data with multiple excitations (i.e., 5 to 6 excitations) and using the averaged signal to improve DW-MRI image quality. However, acquiring multi b-value DW-MRI data with multiple excitations to achieve both sufficient image quality and sufficient information for quantitative assessment of fast and slow diffusion substantially increases acquisition times, making this method less suitable for routine clinical use. A unique feature in DW-MRI images in particular, and in parametric imaging techniques in general, is the addition of a 4th dimension to the control parameters in the acquired data. This 4th parametric dimension, which is the diffusion weighting factor (b-value) at play in DW-MRI, can be exploited as an additional source of prior information that can be utilized in reconstructing images. Recently Freiman et al[2] introduced a novel method to reduce the number of excitations required to obtain multi b-value DW-MRI images of the body with sufficient SNR by introducing a Bayesian model of the expected signal with the signal decay model utilized as the prior information. With this approach, it is possible to simultaneously obtain high-quality multi b-value DW-MRI images and precise estimates of the fast and slow diffusion components. In this work we evaluate the *in-vivo* improvement in multi b-value image quality constructed using the SMEIR approach in both healthy volunteer and Crohn's disease patients' data.

Materials and Methods: We acquired DW-MRI data of a healthy volunteer using a 1.5-T unit (Magnetom Avanto, Siemens Medical Solutions, Erlangen, Germany). We performed free-breathing single-shot echo-planar imaging using the following parameters: repetition/echo time (TR/TE) = 6800/59 ms; matrix size = 192×156; field of view = 300×260 mm; slice thickness/gap = 5 mm/0.5 mm; 40 axial slices; 7 b-values = 0,50,100,200,400,600,800 s/mm^2 with 6 excitations (i.e. NEX=6). The acquisition time for each excitation was 3:30 min. with an overall acquisition time of 21 min. We generated high-quality images by averaging the data from the 6 excitations and 6 low-quality datasets - each one consisting of data acquired with 1 NEX. For each low-quality dataset, we reconstructed the images using our SMEIR reconstruction approach. For purposes of evaluation, we defined 2 spherical regions of interest (ROI) in the liver and in the kidney, respectively. We defined SNR at each voxel as the average signal over the 6 low-quality datasets divided by the standard deviation\ of the signal over these datasets. We likewise calculated SNR for the b-value=800 s/mm^2 DW-MRI image for the raw low-quality datasets (RAW) and for the SMEIR-reconstructed datasets (SMEIR). Next, we averaged SNR for the RAW and SMEIR data, respectively, over the liver and kidney ROIs.

To demonstrate the actual clinical impact of using our SMEIR reconstruction approach instead of the raw low-quality DW-MRI data, we assessed the conspicuity of inflamed bowel regions in b-value=800 s/mm^2 images by means of contrast to-noise ratio (CNR) between regions with active inflammation and surrounding normal tissues in DW-MRI data of Crohn's disease patients. We retrospectively reviewed DW-MRI data of 30 patients who underwent clinical MRI exams including MR enterography (MRE) that included polyethylene glycol administration for bowel distention; gadolinium-enhanced, dynamic 3D VIBE (volume-interpolated breath hold exam); and DW-MRI with the same protocol described above acquired with 1 NEX. Two radiologists reviewed the MRE data independently. Disease activity was defined as abnormal bowel wall thickening and enhancement in the gadolinium-enhanced images by each of the readers. In case of disagreement between the two reviewers, consensus was reached by joint reading of the data. The consensus decision identified 12 patients with active inflammation in the ileum. Another radiologist, blinded to the MRE data and to the review, identified the ileum on the DW-MRI data for each patient. We manually annotated the ileum wall on the DW-MRI images with b-value=200 s/mm^2. Next, we calculated the CNR of the inflamed ileum in b-value=800 s/mm^2 images by subtracting the background signal from the signal of the inflamed ileum and dividing by the standard deviation of the signal in the ileum.

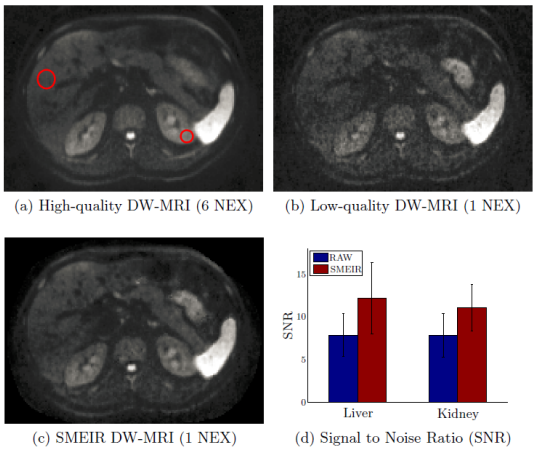

Fig. 1: In-vivo example. This figure presents b-value=800 s/mm^2 images acquired in high-quality (NEX=6); in low-quality (NEX=1); and in low-quality (NEX=1) combined with SMEIR reconstruction, and a bar-plot representation of SNR of low-quality data with and without SMEIR reconstruction.

Results: Fig. 1 presents a high b-value (i.e. 800 s/mm^2) image of the healthy volunteer acquired in high-quality (NEX=6); in low-quality (NEX=1); in low-quality (NEX=1) combined with SMEIR reconstruction; and a bar-plot representation of SNR of low-quality data with and without SMEIR reconstruction. The average±std SNR of SMEIR data (12.2±2.5 in the liver and 11±2.5 in the kidney) was higher than the SNR of the low-quality data (7.9±4.2 in the liver and 7.8±2.7 in the kidney) - a difference that was statistically significant (Paired Student's t-test, $p<0.0001$). Notably, the SMEIR reconstruction of low-quality data improved SNR substantially without additional acquisition time.

Fig. 2 depicts the acquired raw DW-MRI data and SMEIR-reconstructed data of a representative Crohn's disease patient with active inflammation in the ileum. Visually, the region with active inflammation is more conspicuous in the SMEIR-reconstructed image than in the raw DW-MRI data. Quantitatively, the average (std) CNR between the inflamed regions and the surrounding neighborhood in the SMEIR-reconstructed images was higher (2.52±0.69) than in the raw DW-MRI data (2.23±0.47) - a difference that was statistically significant (Paired Student's t-test, $p<0.05$). The SMEIR-reconstructed images improved CNR by 12.6%.

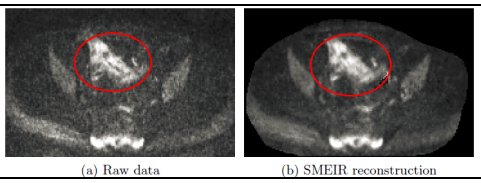

Fig. 2: Representative Crohn's disease patient with active inflammation in the ileum. (a) The acquired raw DW-MRI data; and (b) SMEIR-reconstructed data. The region with active inflammation is more conspicuous in the SMEIR-reconstructed image.

Discussion: We have presented the impact of the new SMEIR model and method for reconstructing high-quality multi b-value DW-MRI images of the body without increasing overall acquisition times. This novel approach features the signal decay model as a priori knowledge in the image reconstruction, effectively enabling us to simultaneously reconstruct DW-MRI images and estimate the signal decay model parameters. The SMEIR method improves overall image quality by increasing the signal-to-noise ratio (SNR) and by increasing the conspicuity of inflamed bowel regions of pediatric Crohn's disease patients without increasing overall acquisition times. The proposed method permits the acquisition of high-quality DW-MRI images for diagnostic purposes within a clinically acceptable acquisition timeframe.

Bibliography:

1. Koh DM, Collins DJ, Orton MR. AJR Am J Roentgenol. 2011 Jun;196(6):1351-61.
2. Freiman M, Perez-Rossello JM, Callahan MJ, Voss SD, Mulkern RV, Warfield SK. Med Image Comput Comput Assist Interv. 2013;16(3):1-8.